J. Fluid Mech. (1973), *vol.* 61, *part* 2, *pp.* 289–299
Printed in Great Britain

Pipe flow measurements of turbulence and ambiguity using laser-Doppler velocimetry

By N. S. BERMAN
School of Engineering, Arizona State University, Tempe
AND J. W. DUNNING
N.A.S.A. Lewis Research Center, Cleveland, Ohio

(Received 7 May 1973)

The laser-Doppler ambiguities predicted by George & Lumley have been verified experimentally for turbulent pipe flows. Experiments were performed at Reynolds numbers from 5000 to 15 000 at the centre-line and near the wall. Ambiguity levels were measured from power spectral densities of FM demodulated laser signals and compared with calculations based on the theory. The turbulent spectra for these water flows after accounting for the ambiguity were equivalent to hot-film measurements at similar Reynolds numbers. The feasibility of laser-Doppler measurements very close to the wall in shear flows is demonstrated.

1. Introduction

Any analysis of a laser-Doppler signal from a single-scattering volume in a turbulent flow to obtain velocity correlations and power spectral densities has inherent limitations. George & Lumley (1973) present a theoretical treatment of these limitations and experimental confirmation using turbulent flow behind a grid where turbulence intensities are low. We have made measurements using an FM demodulator at several radial positions in pipe flows with turbulence intensities as high as 17 % of the local flow velocity. The ambiguities predicted by George & Lumley show up convincingly, but the power spectral density can still be obtained up to wavenumbers as large as those for hot-film anemometers.

2. Description of the apparatus

The laser-Doppler velocimeter used in this work is a one-dimensional instrument with a reference-beam optical arrangement of the Goldstein–Kreid type (1967) as sketched in figure 1. A scattering angle of approximately 9·9° measured in water was used along with a Bragg tank which gave a static frequency shift of 30 MHz (zero velocity corresponds to 30 MHz). The Bragg tank was made from a 5 cm diameter X-cut quartz crystal polished for fifth-overtone operation at 30 MHz. It was used to avoid noise problems at low frequencies. The laser was a Spectra Physics Model 125. The component of the scattering wave vector (we define the scattering wave vector **K** as the difference between the reference- and scattered-beam wave vectors) in the direction of measurement was 7250 Hz/(cm/s).

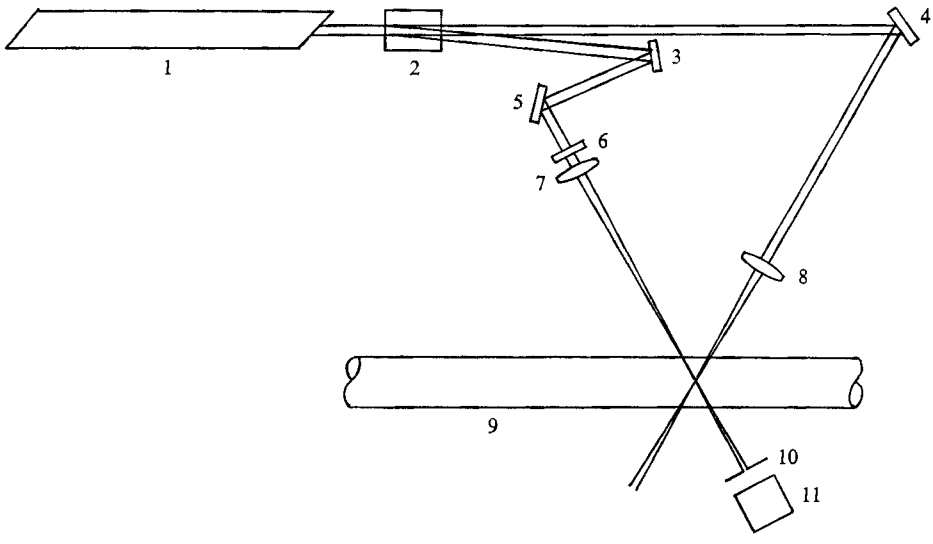

FIGURE 1. Sketch of the optical arrangement. (1) Laser. (2) Bragg tank to shift the frequency of the reference beam. (3)–(5) Mirrors. (6) Neutral density filter. (7) Lens of long focal length on the reference beam. (8) Lens of short focal length which defines the scattering volume (see table 1 for list). (9) Transparent pipe. (10) Pinhole. (11) Photomultiplier tube.

The frequency spectrum of the photomultiplier signal could be directly displayed on a Hewlett–Packard 8553 spectrum analyser. Alternatively the photomultiplier signal could be mixed with a signal from a local oscillator and the difference sent to an FM demodulator. Two different demodulators were used: a fixed centre frequency, phase lock loop (EMR Model 167) and a tunable discriminator (EMR 4140 with a five-pole Bessel low-pass output filter) which used pulse averaging demodulation.

The flow system was a recirculating water unit with an automatic level control on the head tank. The level in the tank could be controlled to within $\pm 1{\cdot}5$ mm. This is equivalent to a $0{\cdot}1\,\%$ control of the total head. Glass pipes 1·9 cm, 2·54 cm and 5·08 cm in diameter were used in the test section and measurements were made approximately 300 cm downstream of an entrance section. Water containing a small amount of $0{\cdot}5\,\mu$m polystyrene spheres was used in the system.

Analysis of the spectrum analyser display and a further description of the apparatus has been published previously (Dunning & Berman 1972). Spectrum analyser averages give information corresponding to the probability distribution of frequency.

FM demodulation techniques can be used to yield signals which can be processed to obtain autocorrelations and power spectra of the fluctuations. In our demodulation technique optical heterodyning of the scattered and reference beams at the photomultiplier tube gave a frequency shift Δf proportional to the instantaneous velocity $\overline{U}+u$. This fluctuating frequency was heterodyned with a constant frequency f to move the signal to $|f-\Delta f|$, the centre frequency of the FM demodulator. To track the turbulence signals at the various intensity levels, the output filter was changed when the phase lock loop was used and both the

centre frequency and the tracking range were changed when the tunable discriminator was used. The demodulated output, after passing through a low-pass filter, was a voltage proportional to the fluctuating velocity u. This voltage was recorded on an FM tape recorder. All tests were recorded at 15 in./s on a Precision Instrument Co. Model 207 tape recorder except 6(a) and 6(b), which were recorded at 60 in./s. Alternate channels of the seven-channel 0·5 in. tape were left blank to improve the signal-to-noise ratio. Later the tape was played back into an analog-to-digital converter which digitized the fluctuating voltage signal and made a digital tape. In the analog-to-digital conversion, 13 bits were available to convert -10 to $+10$ V to digital numbers from 0 to 8192. The digital tapes were processed on an IBM 360/67 computer to obtain power spectra, autocorrelations and probability distributions.

For purposes of digital analysis, the data were divided into two regions: (i) below 100 Hz, digitized at 1000 points/s for 16 s; (ii) above 100 Hz, digitized at 8000 points/s for 2 s. The autocorrelation and power spectral density were obtained using fast Fourier transform techniques. In most cases 128 lagged products equally spaced in frequency were obtained after averaging the raw spectra using a 'Parzen Window'. Details of the computer program 'Rapsody' and the averaging technique can be found in the report of Brumbach (1968). The spacing of the averaged data points was every 4 Hz for the 1000 points/s rate and every 32 Hz for the higher rate. The 'probable errors' are estimated to be 21 % at the lowest frequency, 4 Hz, and 12 % at 100 Hz. To examine further the shape of the ambiguity, the runs designated 6(a) and 6(b) in tables 2 and 3 were digitized at 16 000 points/s for 1s and tables of 1024 and 128 lagged products were calculated. For the curves reported in this work smooth lines are drawn through the closely spaced data points.

In the remainder of this paper we describe results in terms of two different spectra. To avoid confusion we note here that in § 3 we refer only to the spectrum analyser spectra (the spectra of the raw signal from the photomultiplier tube) while in § 4 we consider only the power spectral density of the fluctuations (the power spectral density of the output signal from the phase lock loop). Both spectra contain the ambiguities: in the spectrum analyser spectra as a broadening and in the power spectra as additional high frequency noise.

As a test of the noise level of the tape recorder system and the roll-off of the low-pass filter, a signal frequency-modulated by white noise was made the input to the FM demodulator and processed as described. The white-noise signal level on the power spectrum was 250 mV^2/Hz while the tape recorder noise beyond the filter cut-off of 500 Hz was 0·1 mV^2/Hz or less. For the measurements in turbulent flows reported herein the ambiguity levels were always greater than 10 mV^2/Hz, well above the tape recorder noise. Since we were primarily interested in the ambiguity at frequencies in the neighbourhood of 500 Hz this test establishes the validity of the ambiguity measurements better than an overall signal-to-noise ratio criterion.

3. Determination of the scattering volume

From a laminar flow analysis of the laser-Doppler velocimeter the standard deviation of the finite volume broadening can be used to determine the size of the sample volumes in the axial direction and in the radial direction, σ_x and σ_z, respectively. These dimensions used here are defined by Edwards *et al.* (1971) and must be multiplied by $\sqrt{2}$ to get the equivalent scattering-volume size as given by George & Lumley.† The variance of the frequency spectrum as measured with a spectrum analyser of the scattered radiation from particles in laminar flow is

$$V = \frac{U_0^2}{4\sigma_x^2} + \left(K\frac{dU}{dz}\right)_0^2 \sigma_z^2 + \frac{1}{2}\left(K\frac{\partial^2 U}{\partial z^2}\right)_0^2 \sigma_z^4 + O(\sigma_z^2/\sigma_x^2), \tag{3.1}$$

where the subscript 0 refers to the centre of the scattering volume. Here K is the x component of the scattering wave vector in units of cm^{-1} and $U(z)$ is the x component of velocity:

$$U(z) = U_0 + \left(\frac{\partial U}{\partial z}\right)_0 (z - z_0) + \left(\frac{\partial^2 U}{\partial z^2}\right)_0 \frac{(z-z_0)^2}{2} + \ldots . \tag{3.2}$$

Equation (3.1) is obtained by using (3.2) in the equation for the autocorrelation of the photodetector current for flows with spatial velocity variation [Edwards *et al.* 1971, equation (53)]. The variance of the spectrum of the photodetector current is easily found from the second derivative of the autocorrelation with respect to the time displacement since the autocorrelation is the Fourier transform of the spectrum.

The higher order terms can be neglected for small scattering angles but for completeness the next two terms in the variance are

$$\frac{\sigma_z^2}{4\sigma_x^2}\left(\frac{\partial U}{\partial z}\right)_0^2 + U_0\left(\frac{\partial^2 U}{\partial z^2}\right)_0 + \frac{3}{16}\frac{\sigma_z^2}{\sigma_x^2}\left(\frac{\partial^2 U}{\partial z^2}\right)_0^2.$$

For laminar pipe flow

$$U(z) = U_{\max}[1 - (z/R)^2], \tag{3.3}$$

where R is the pipe radius. Then (3.1) becomes

$$V = \frac{U_0^2}{4\sigma_x^2} + 2K^2 U_{\max}^2 \left(\frac{\sigma_z}{R}\right)^2 \left(\frac{\sigma_z}{R}\right)^2 + 2\left(\frac{z}{R}\right)^2, \tag{3.4}$$

where z and U_0 are values at the centre of the scattering volume and $U_{\max}$ the velocity at the centre of the circular pipe. The first term will be called finite transit time broadening $(\Delta\omega_F)^2$, and the second gradient broadening $(\Delta\omega_G)^2$. This equation has been discussed in detail by Edwards *et al.* (1971). We present it here because it is critical to our definition of scattering-volume dimensions. These dimensions were determined by measuring the variance of the spectrum of scattered radiation at the centre and at locations near the wall for laminar

† The difference is that Edwards *et al.* and this work use an analysis for a one-beam system (focusing of only the scattered beam). George & Lumley use a two-beam velocimeter (focusing of both local oscillator and scattered beams.) The optical system shown in figure 1 reduces to this one-beam system when the focal length of lens 7 is much greater than that of lens 8 and the receiving optics consist of a pinhole.

Nominal focal length (cm)	σ_x (μm)	σ_z (μm)
3·75	3	15
15	7	140
50	20	400

TABLE 1

flow. We can then find the σ_x and σ_z which best fit (3.4). For lenses of focal length less than 25 cm and pipe diameters greater than 1 cm, the gradient broadening is negligible at the centre, and the calculation of σ_x and σ_z is simple. Lenses of longer focal length give comparable transit times and gradient broadening at the centre, but near the wall the gradient broadening dominates. It is difficult to calculate the σ_x and σ_z from the geometry, since the optical components are seldom aligned perfectly. The results of 6–20 measurements for the three lens systems of this work are given in table 1.

4. Turbulence measurements

If we assume scattering to be from single particles or the sums of contributions from single particles with no correlation, we can expand $U(\mathbf{r},t) = \overline{U}(\mathbf{r}) + u(\mathbf{r},t)$ to obtain an equation for turbulence similar to (3.1). The overbar represents the customary time average. Edwards, Angus & Dunning (1973) have essentially done this and found additional terms due to turbulent fluctuations $\overline{(\mathbf{K}.\mathbf{u})^2}$, and the turbulent finite transit time, $\overline{u^2}/4\sigma_x^2$. A turbulent term corresponding to the second term on the right-hand side of (3.1) does not appear for homogeneous isotropic turbulence. However, when the light scattered from several particles within the scattering volume is correlated, such a term does appear as shown by George & Lumley. This arises when the Kolmogorov microscale is of the same order as σ_z. For homogeneous isotropic turbulence this additional source of broadening, which we shall call $\Delta\omega_\epsilon$, is approximated from equation (3.2.8) of George & Lumley as

$$(\Delta\omega_\epsilon)^2 \cong 2K^2 \overline{\left(\frac{\partial u}{\partial z}\right)^2} \sigma_z^2 = \frac{4\sigma_z^2}{15} K^2 \left(\frac{\epsilon}{\nu}\right), \tag{4.1}$$

where ϵ is the rate of dissipation of turbulent energy per unit mass and ν is the kinematic viscosity. When $2\sigma_z$ is greater than three times the Kolmogorov microscale, $\Delta\omega_\epsilon$ calculated by (4.1) is too large. George & Lumley show how to correct $\Delta\omega_\epsilon$ and we assume that their approximation can be used for pipe flow.

The other significant contributions to the ambiguity for turbulent pipe flow are from (3.1), in Hz,

$$\Delta\omega_F = \overline{U}/4\pi\sigma_x, \tag{4.2}$$

$$\Delta\omega_G = K(-d\overline{U}/dz)\,\sigma_z, \tag{4.3}$$

where K, in units of Hz/(cm/s), is again the x component of the scattering vector.

We have measured the one-dimensional power spectral density in ten separate

Test	$\overline{U}$ (cm/s)	$\overline{(u^2)}^{\frac{1}{2}}$ (cm/s)	U_* (cm/s)	D (cm)	ϵ (cm^2/s^3)	Lens	$\Delta\omega_F$ (Hz)	$\Delta\omega_G$ (Hz)	$\Delta\omega_\epsilon$ (Hz)	0·73$\Delta\omega$ (Hz) Calculated	0·73$\Delta\omega$ (Hz) Measured
1(*a*)	28·1	1·1	1·5	1·9	7	3·75	7400	0	160	5400	5200
2(*a*)	20·6	0·9	1·1	1·9	2·8	15	2300	0	930	1850	2000
3(*a*)	27·5	1·1	1·5	1·9	7	50	1100	0	3700	2750	2400
4(*a*)	54	2·1	2·6	2·54	27	3·75	14300	0	310	10400	10000
5(*a*)	54	2·1	2·6	2·54	27	15	6000	0	2900	4900	4200
6(*a*)	24·5	0·85	1·0	5·08	1	15	2800	0	490	2100	2500

TABLE 2

Test	$\overline{U}$ (cm/s)	$\overline{(u^2)}^{\frac{1}{2}}$ (cm/s)	y/R	U_* (cm/s)	ϵ (cm^2/s^3)	$-d\overline{U}/dr$ (s^{-1})	U_*y/ν	$\Delta\omega_F$ (Hz)	$\Delta\omega_G$ (Hz)	$\Delta\omega_\epsilon$ (Hz)	0·73 $\Delta\omega$ (Hz) Calculated	0·73 $\Delta\omega$ (Hz) Measured
1(*b*)	25·8	2·0	0·2	1·6	50	22	35	6800	240	430	5000	4900
2(*b*)	26	2·0	0·2	1·7	71	24	36	3000	2400	4700	4600	4800
3(*b*)	21	1·34	0·16	1·5	65	40	25	1000	12000	11000	11900	12500
6(*b*)	23·3	3·7	—	2	440	250	—	2700	33000	11500	25000	23000

TABLE 3

cases where the ambiguities are clearly distinguishable from the turbulent fluctuations. These data are summarized in tables 2 and 3. In the tables y is the distance from the wall, U_* the friction velocity, D the pipe diameter and r the radial co-ordinate. Tests 1–3 were performed with a 1·9 cm diameter pipe at a Reynolds number based on average velocity of about 5000 and the EMR 167 was the demodulator. Tests 4 and 5 involved a 2·54 cm diameter pipe at a Reynolds number of 12000 and test 6 a 5·08 cm diameter pipe at a Reynolds number of 15000. The EMR 4140 tunable discriminator was used for tests 4–6. Table 2 presents a summary of data from the centre-line. Calculated values of the broadening $\Delta\omega_F$, $\Delta\omega_G$ and $\Delta\omega_\epsilon$ are based on the pipe flow parameters given in the table. The (*b*) series in table 3 consists of the results near the wall. Each (*b*) test was made with the same lens as the (*a*) test and at the smallest distance from the wall at which the FM demodulator could respond to the fluctuations from the mean of at least four times the root-mean-square fluctuation. From probability analyses of the velocity fluctuations in pipe flows we find that the probability of a velocity at this deviation from the mean is less than 0·005 of the probability of the mean velocity. The various distances from the wall are the result of using different centre frequencies on the FM demodulators.

Test 6(*b*) was set up by moving the scattering volume towards the wall with the centre-line velocity of test 6(*a*) until the signal was lost. Then the velocity was increased until a suitable signal could be electronically processed. The spectrum analyser trace gave a standard deviation $\Delta\omega$ of 5·2 cm/s, however, the r.m.s. turbulence from the demodulated spectra was 3·7 cm/s. The exact location of the scattering volume for test 6(*b*) was not known closely enough to estimate the broadening so values at the edge of the viscous sublayer corresponding to a $U_* y/\nu$ of 10 are given in the table.

The $\Delta\omega_F$, $\Delta\omega_G$ and $\Delta\omega_\epsilon$ in tables 2 and 3 are calculated from (4.1), (4.2) and (4.3). Then

$$\Delta\omega = (\Delta\omega_F^2 + \Delta\omega_G^2 + \Delta\omega_\epsilon^2)^{\frac{1}{2}}. \tag{4.4}$$

We have obtained the dissipation ϵ from Laufer's (1954) measurements and the mean gradient was estimated from Eckelmann (1970), both at the equivalent $U_* y/\nu$ for the wall data. From Rice (1948) and George & Lumley (1973) the ambiguity should be $0{\cdot}73\Delta\omega$ for spectra defined only for positive frequencies. George & Lumley define their spectra over both positive and negative frequencies, leading to an additional factor of 0·5. The last two columns in the tables compare the calculated ambiguity levels with the measured levels from power spectra of the demodulated signal.

The tabulated results show the influence of scattering-volume size and velocity gradient on the ambiguity. When finite transit time is the major ambiguity as in all the (*a*) tests except 3(*a*), $\Delta\omega$ depends on σ_x and the mean velocity only. The experimental results agree almost exactly with the theory. Test 3(*a*), with a large scattering volume in the z direction, has mostly turbulent ambiguity. Again the agreement with theoretical calculations is excellent. It should be noted here that the errors in using a spectrum analyser without correction for ambiguity are 35 % for the 3·75 cm lens, 6 % for the 15 cm lens and 10 % for the 50 cm lens. The 15 cm lens is near the optimum for these low Reynolds number flows.

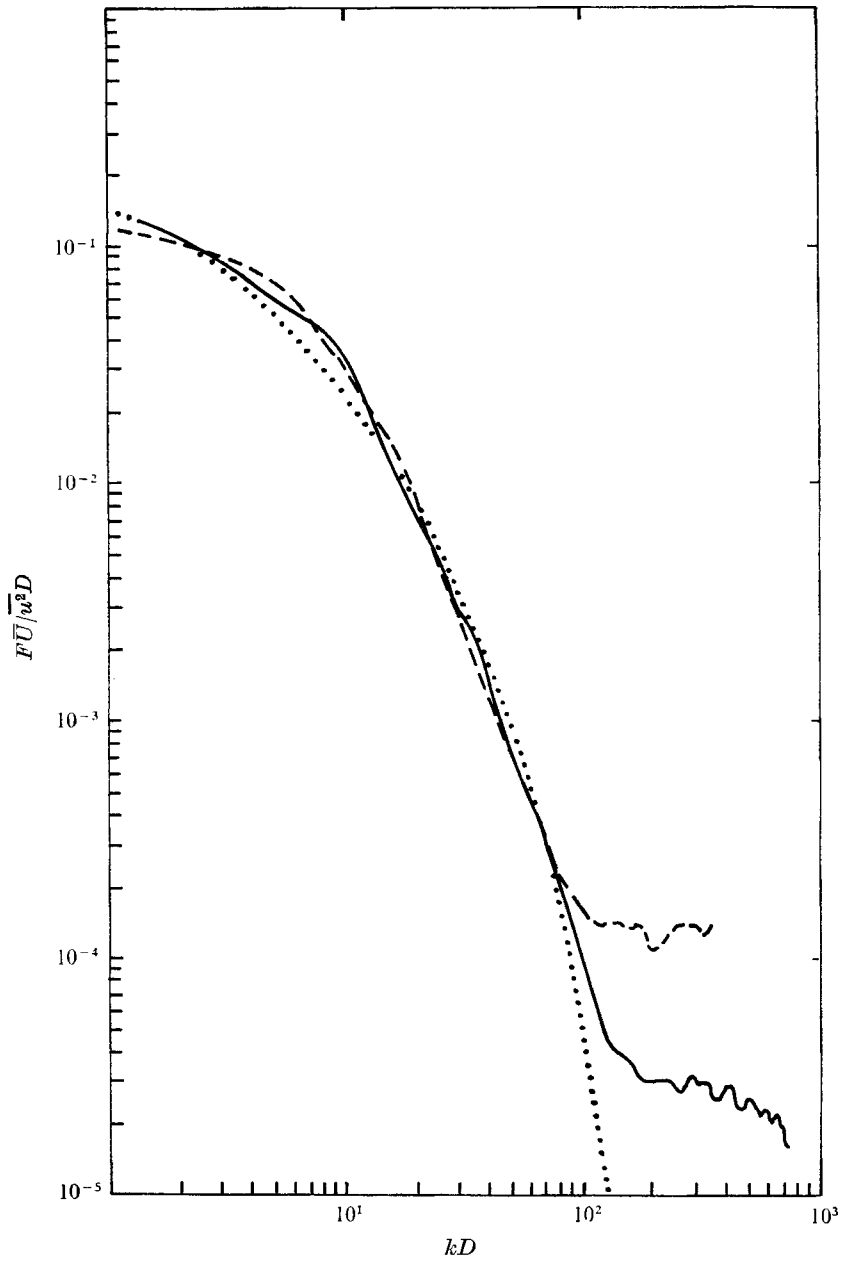

FIGURE 2. Normalized power spectral density of velocity fluctuations for laser-Doppler pipe flow tests 4(*a*) (broken line) and 5(*a*) (solid line) and a hot-film test of Resch & Coantic (1969) (dotted line), all at a local Reynolds number of 15000. F is the power spectral density in cm^2/s and k the wavenumber $2\pi f/\overline{U}$. The ambiguity cut-off due to finite transit time broadening is shown.

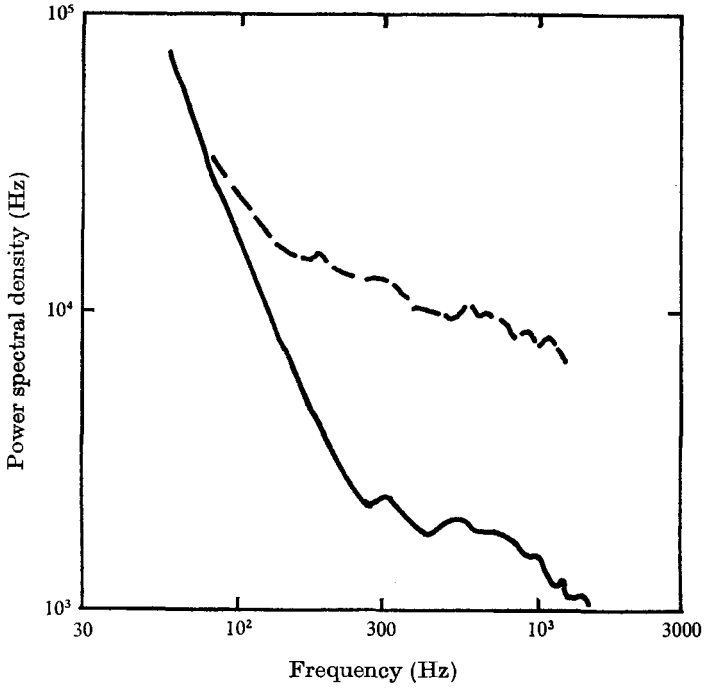

FIGURE 3. Power spectra at high frequencies showing turbulent ambiguity cut-off for tests 3(*a*) (solid line) and 3(*b*) (broken line).

Near the wall the lens of shortest focal length becomes more desirable as shown in table 3. Tests 2(*b*) and 3(*b*) contain significant gradient and turbulent ambiguity. At the edge of the sublayer the variance of the spectrum analyser spectrum contains comparable components from turbulence intensity and ambiguity as can be seen by comparison of $K(\overline{u^2})^{\frac{1}{2}}$ with $\Delta\omega$ for tests 3(*b*) and 6(*b*). If the lens of focal length 3·75 cm is used, the ambiguity can be reduced by approximately a factor of 2.

The dependence of the power spectra on frequency is also of interest. Typical normalized power spectral density plots for the centre-line for two different lenses are shown in figure 2, corresponding to tests 4(*a*) and 5(*a*). The turbulence portions of the spectra are seen to agree closely with the recent hot-film results of Resch & Coantic (1969) at the equivalent local Reynolds number. The ambiguity appears as the level portion at the lower right of the figure, resulting in a loss of turbulence information at high frequencies. The laser-Doppler curve falls onto the hot-film curve when the ambiguity is subtracted. Over the range of frequencies in which the ambiguity appears it should show up as essentially flat and slightly decreasing at higher frequencies. The Bessel filter in the demodulator is responsible for the fluctuations in the ambiguity observed in figure 2 and the tape recorder filter is responsible for the fall-off at frequencies above $kD = 500$. The lens of focal length 15 cm represents the optimum case as previously explained. We can compare such spectra with the ambiguity theory by plotting the power spectral density in units of Doppler-shift frequency deviation from

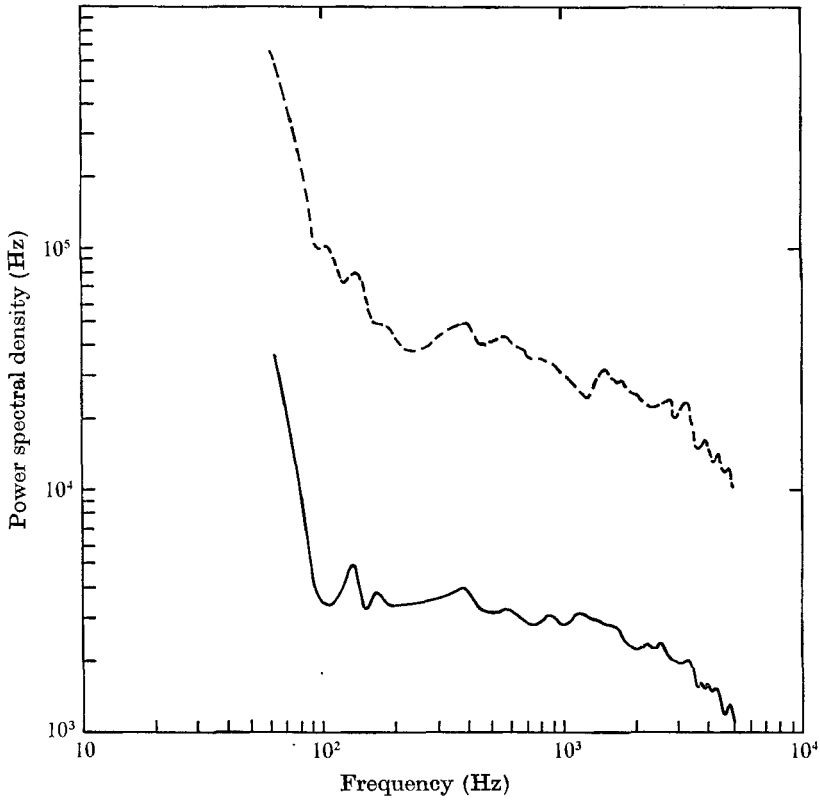

FIGURE 4. Power spectra at high frequencies for tests 6(*a*) (solid line) and 6(*b*) (broken line). Finite transit time broadening, test 6(*a*), and velocity gradient broadening, test 6(*b*), are compared.

the mean square divided by frequency bandwidth. This is easily obtained from K and any gains in the electronic analysis. We estimated the ambiguity levels from plots similar to figure 2, and these are listed under '$0{\cdot}73\Delta\omega$, measured', in tables 2 and 3.

Examples of the turbulent ambiguity are shown in figure 3, corresponding to tests 3(*a*) and 3(*b*), the lens of longest focal length. The turbulent ambiguity dominates both at the centre-line and near the wall for this lens. Finally, figure 4 shows centre-line and wall spectra for the lens of focal length 15 cm. The finite transit time ambiguity at the centre-line and the gradient ambiguity near the wall both appear as essentially white noise.

We have omitted any contribution from the curvature of the mean profile in our calculations. For the worst case, test 3(*b*), this amounts to 3000 Hz, which is less than a 4 % increase in the gradient broadening.

5. Conclusions

The theory of George & Lumley has been confirmed with respect to the magnitude of the ambiguity and the sources of ambiguity. The ambiguity spectrum was also found to be essentially flat or equivalent to white noise over the range of measurements for all forms of broadening.

We see from figure 2 that the laser-Doppler velocimeter with a continuous signal can be used to obtain pipe flow turbulence data equivalent to that from a hot-film anemometer. However, interpretation of these data must take into account the ambiguities inherent in the instrument. The complete measurement of the spectrum shows the ambiguity clearly while probability and correlation data would be more difficult to interpret.

We have also shown measurements in pipe flow near the edge of the viscous sublayer at low turbulent Reynolds numbers. The optimum scattering volume for measurements near the wall was found to be different from the optimum at the pipe centre-line.

REFERENCES

BRUMBACH, R. P. 1968 *Digital Computer Routines for Power Spectral Analysis.* Santa Barbara, California: A. C. Electronics.

DUNNING, J. W. & BERMAN, N. S. 1972 *Symp. on Turbulence in Liquids, University of Missouri, Rolla,* TMX-67969.

ECKELMANN, H. 1970 An experimental investigation in a turbulent channel flow with a thick viscous sublayer. *Max-Planck Inst. Fluid Mech., Göttingen, Rep.* no. 48.

EDWARDS, R. V., ANGUS, J. C. & DUNNING, J. W. 1973 *J. Appl. Phys.* **44**, 1694–1698.

EDWARDS, R. V., ANGUS, J. C., FRENCH, M. J. & DUNNING, J. W. 1971 *J. Appl. Phys.* **42**, 837–850.

GEORGE, W. K. & LUMLEY, J. L. 1973 *J. Fluid Mech.* **60**, 321.

GOLDSTEIN, R. J. & KREID, D. K. 1967 *J. Appl. Mech.* E **34**, 813.

LAUFER, J. 1954 The structure of turbulence in fully developed pipe flow. *N.A.C.A. Tech. Rep.* no. **1174**.

RESCH, F. & COANTIC, M. 1969 *Houille Blanche,* **24**, 151.

RICE, S. O. 1948 *Bell Syst. Tech. J.* **27**, 109–157.